Supplementary Information

Atom-scale dispersed palladium in conductive $Pd_{0.1}TaS_2$ lattice with unique electronic structure for efficient hydrogen evolution

Dong Wang,[a,‡] Xin Wang,[b,‡] Yue Lu,[c,‡] Changsheng Song,[a] Jie Pan,[a] Chilin Li,[a] Manling Sui,[c,*] Wei Zhao,[a,*] and Fuqiang Huang[a,b,*]

[a] State Key Laboratory of High Performance Ceramics and Superfine Microstructures
Shanghai Institute of Ceramics, Chinese Academy of Sciences, 1295 Dingxi Road, Shanghai 200050, P.R. China

[b] State Key Laboratory of Rare Earth Materials Chemistry and Applications and National Laboratory, College of Chemistry and Molecular Engineering, Peking University
No.5 Yiheyuan Road Haidian District, Beijing 100871, P.R. China

[c] Institute of Microstructure and Properties of Advanced Materials, Beijing University of Technology
No.100, Pingleyuan, Chaoyang District, Beijing 100124, P.R. China

Experimental Procedures

Electrocatalytic hydrogen evolution performance: The calibration of potential was following the Equation S1:

$$E_{HER} = E_{applied} + 0.1981 + 0.059 \times pH - i \times R, \quad \text{(S1)}$$

where $E_{applied}$ was the applied potential (*vs.* Ag/AgCl) in 0.5 mol L^{-1} H_2SO_4, R was the compensated resistance, i was the measured current and pH value of 0.5 mol L^{-1} H_2SO_4 was 0. The current densities were normalized by dividing geometric surface areas of rotating disk electrode (0.1963 cm^2).

Tafel analysis: The Tafel equation is an equation in electrochemical kinetics relating the rate of an electrochemical reaction to the overpotential. It was expressed by the following Equation S2:

$$\eta = a + b * log|j|, \quad \text{(S2)}$$

where η is the overpotential (mV), b is the Tafel slope, a is the Tafel constant and j is the current density (mA cm^{-2}).

The most inherent measure of activity for the HER is the exchange current density. It was determined by the Equation S3: [1]

$$\eta = a + b * log|j_0|,$$

(S3)

where η is the overpotential (mV), b is the Tafel slope, a is the Tafel constant and j_0 is the exchange current density (mA cm^{-2}) when the η equals 0.

Active sites measurements: The density of active sites was measured using underpotential deposition (UPD) of copper using the method described by Green[2]. He demonstrated that the active site can be measured by the charges exchanged during copper stripping after deposition at the underpotenial regions. Electrolytes were saturated with Ar prior the measurements. In 0.1 mol L^{-1} H_2SO_4 and 2 mmol L^{-1} of $CuSO_4$ solution, the electrode surface was thoroughly electrochemically cleaned by applying a potential of 673 mV *vs.* RHE for 2 minutes. Cyclic voltamperometric were performed with a scan rate of 2 mV s^{-1} and Ag/AgCl electrode was used as the reference. The potential was lowered first and kept constant for 100 s to deposit copper. After that, it was increased to 673 mV *vs.* RHE to oxidize the copper. Hydrogen adsorption was measured the same way using a 0.1 mol L^{-1} H_2SO_4 solution.

Calculation of Turnover Frequency: The turnover frequency is the intrinsic characteristic of active site for catalytic reaction, assuming all of the active atoms in the catalyst drop-casted on the rotating disk electrode are catalytically active. Turnover frequencies were calculated from the density of active sites using the following Equation S4: [3]

$$TOF = j/(\rho * e * 2), \quad \text{(S4)}$$

where j is the exchange current density, ρ is the density of active sites, e is the quantity of an electric charge and 2 represents the charge of a H_2 molecule.

Table S1. The intercalation compounds and loading hybrid samples for contrast.

Intercalation compound	Loading hybrid
/	TaS_2
$Pd_{0.025}TaS_2$	Pd/TaS_2 (1 *wt.*%)
$Pd_{0.05}TaS_2$	Pd/TaS_2 (2 *wt.*%)
$Pd_{0.1}TaS_2$	Pd/TaS_2 (4 *wt.*%)

Table S2. Crystal data information, data collection strategy and refinement results using Rietveld refinement method.

Space group (Hexagonal)	$P6_3/mmc$
Hall symbol	$-P\ 6c\ 2c$
Crystal parameters (Å)	a = 3.31910 (6) , c = 12.1753 (5)
Cell volume (Å^3)	V = 116.16 (1)
Collected diffraction angle (°) ranges	$2\theta_{min}$ = 5.10°, $2\theta_{max}$ = 94.23°, $2\theta_{step}$ = 0.02°
Radiation source	X-ray radiation
Data points used	4457 data points
Numbers of parameters refined	78
Restraints used	none
R_p	4.866 %
R_{wp}	6.447 %
R_{exp}	4.042 %
R_{Bragg}	2.635 %
χ^2	2.543

Table S3. Elemental compositions of Pd, Ta and S in $Pd_{0.1}TaS_2$ by EDX.

Element	Weight %	Atomic %
Pd	4.19	3.49
Ta	74.06	36.31
S	21.76	60.20

Note: The corresponding accurate chemical formula of $Pd_{0.1}TaS_2$ is $Pd_{0.096}TaS_{1.658}$ based on the EDX data.

Table S4. The Pd and Ta element contents of Pd_xTaS_2 powders by ICP-AES.

Sample	Element	Concentration (mg/L)	Mass fraction of Pd (*wt.* %)	Ratio of Pd to Ta
$Pd_{0.1}TaS_2$	Pd	4.66	4.66	0.063:1
	Ta	73.31		
$Pd_{0.050}TaS_2$	Pd	2.09	2.09	0.035:1
	Ta	59.37		
$Pd_{0.025}TaS_2$	Pd	1.08	1.08	0.018:1
	Ta	58.56		

Note: The mass of Pd_xTaS_2 was 50 mg and dissolved into 500 ml solution.

Table S5. Comparison of the catalytic activity between $Pd_{0.1}TaS_2$ and other catalysts in the literatures.

Catalyst	Onset overpotential (mV)	Tafel slope (mV dec^{-1})	η at the 10 mA cm^{-2} (mV)	Dosage of Pd (*wt.* %)	Reference
$Pd_{0.1}TaS_2$	77	52.7	121	4.36	This work
Pd/TaS_2	114	87.2	412	4.16	This work
TaS_2	295	200.0	/	0.00	This work
Pd/C	264	124.0	398	20.00	[4]
Pd nanodots/defect-rich MoS_2	40	41.0	103	10.58	[4]
Pd nanodots	249	59.0	249	100.00	[4]
TaS_2	488	93.4	/	0.00	[5]
Pt nanoparticles/TaS_2 nanosheet	95	54.0	182	Not mentioned	[5]

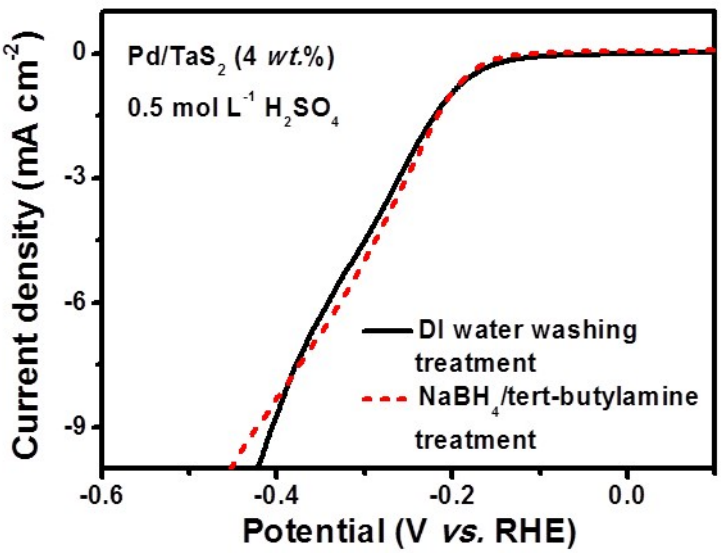

Figure S1. The HER performances of Pd/TaS_2 samples (4 *wt.*%) using the DI water washing treatment and $NaBH_4$/tert-butylamine treatment, respectively.

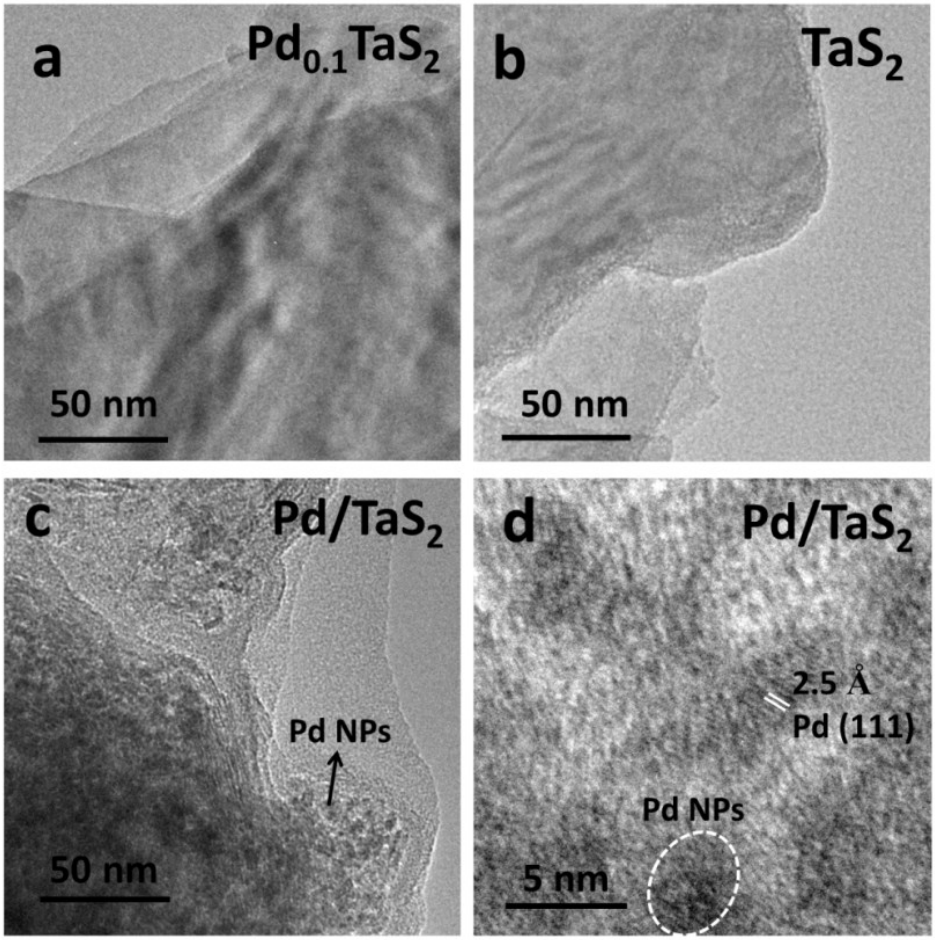

Figure S2. (**a**) TEM image of $Pd_{0.1}TaS_2$; (**b**) TEM image of TaS_2; (**c**) TEM image of Pd/TaS_2 (loading mass of *4 wt.* %) hybrid; (**d**) HRTEM of the Pd/TaS_2 (loading mass of *4 wt.* %) hybrid.

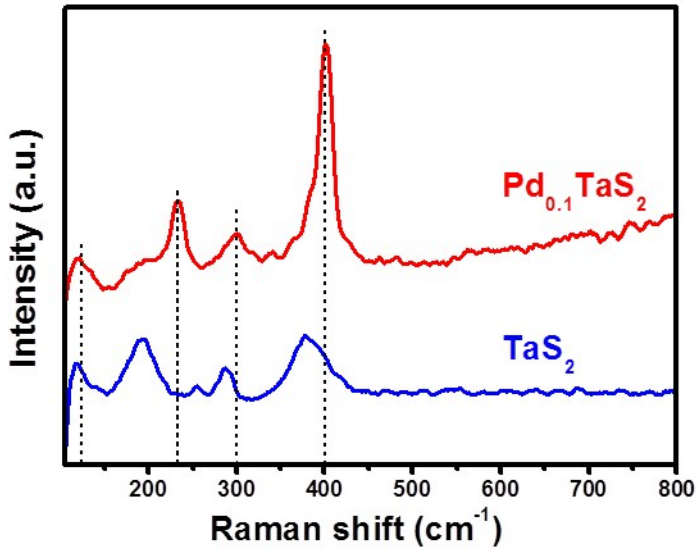

Figure S3. The Raman spectra of $Pd_{0.1}TaS_2$ and TaS_2 as a comparison.

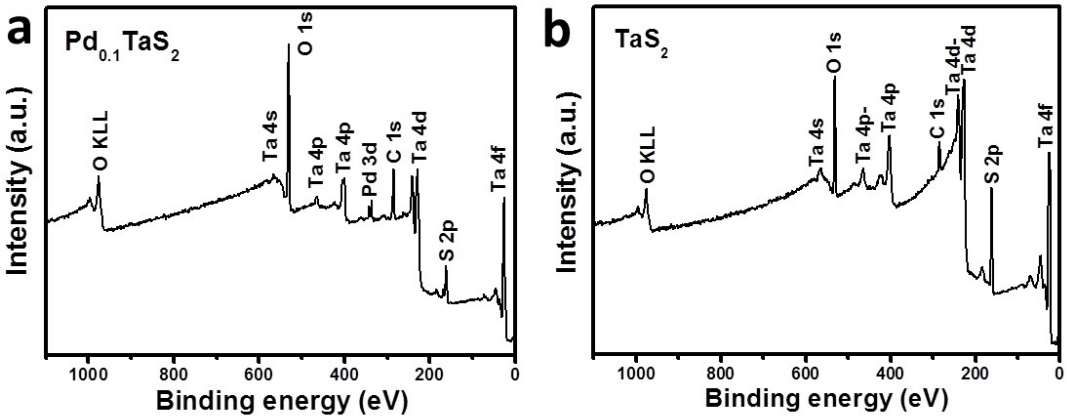

Figure S4. XPS spectrum of $Pd_{0.1}TaS_2$ and TaS_2.

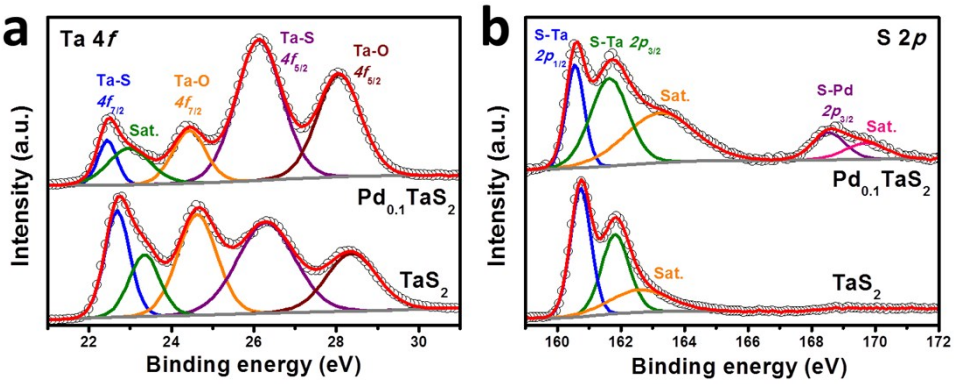

Figure S5. XPS spectrum of Ta 4*f* (**a**) and S 2*p* (**b**) for $Pd_{0.1}TaS_2$ and TaS_2.

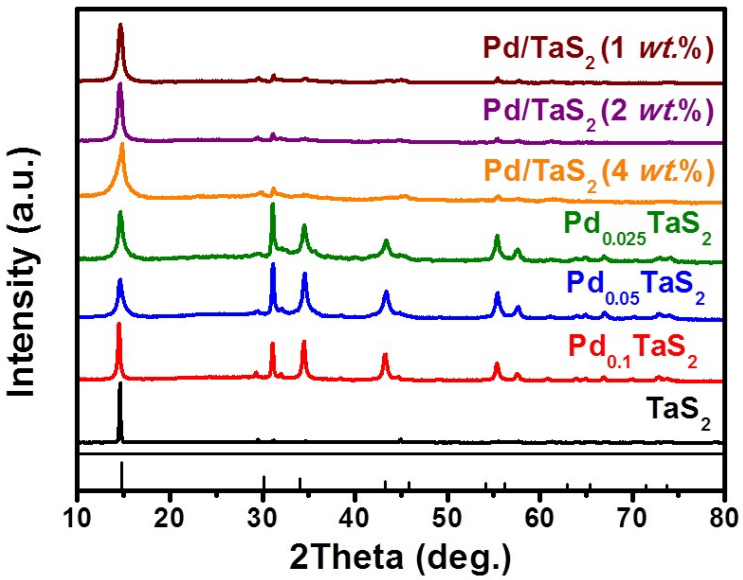

Figure S6. The XRD patterns of Pd_xTaS_2, the respective Pd/TaS_2 hybrids and pure TaS_2.

Patterns of TaS_2 standard is shown at the bottom.

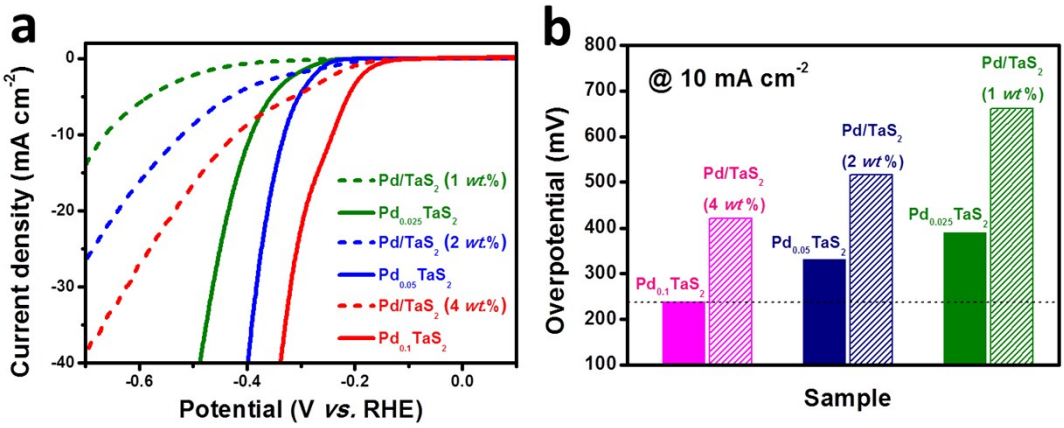

Figure S7. HER electrocatalytic properties of Pd_xTaS_2 samples and Pd/TaS_2 hybrids. (**a**) Polarization curves of Pd_xTaS_2 and the respective Pd-loaded TaS_2 hybrid samples; (**b**) the overpotential of Pd_xTaS_2 and the respective Pd NPs on TaS_2 at the current density of 10 mA cm^{-2}.

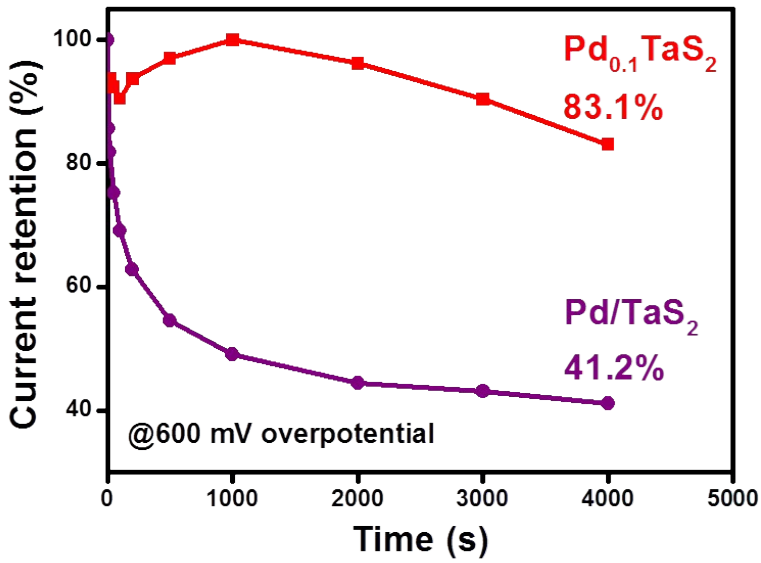

Figure S8. The stability of $Pd_{0.1}TaS_2$ and Pd/TaS_2 (4 *wt.* %) at the overpotential of 600 mV for 4000 s using chronoamperometry.

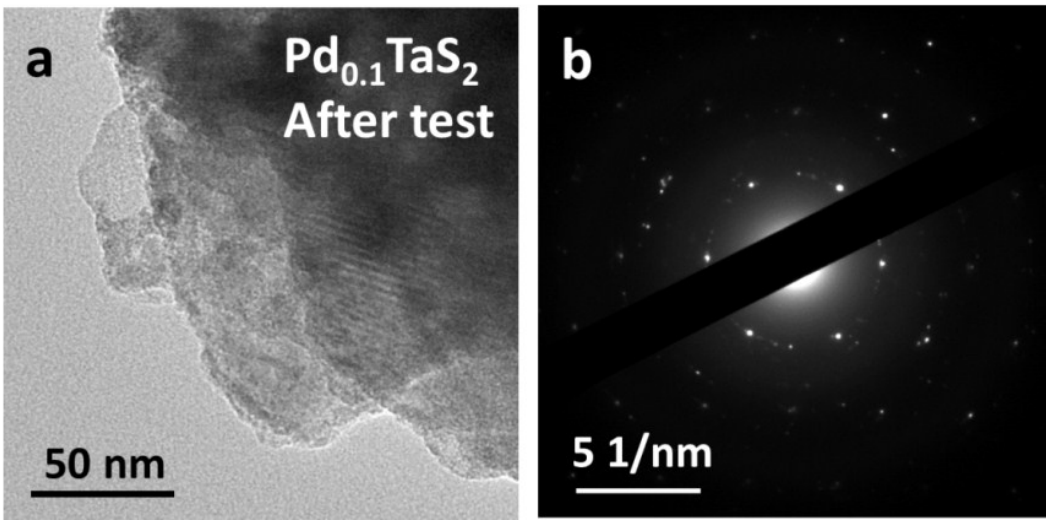

Figure S9. (**a**) TEM image of $Pd_{0.1}TaS_2$ catalyst at the overpotential of 600 mV for 4000 s; (**b**) the corresponding selected area electron diffraction pattern (SAED).

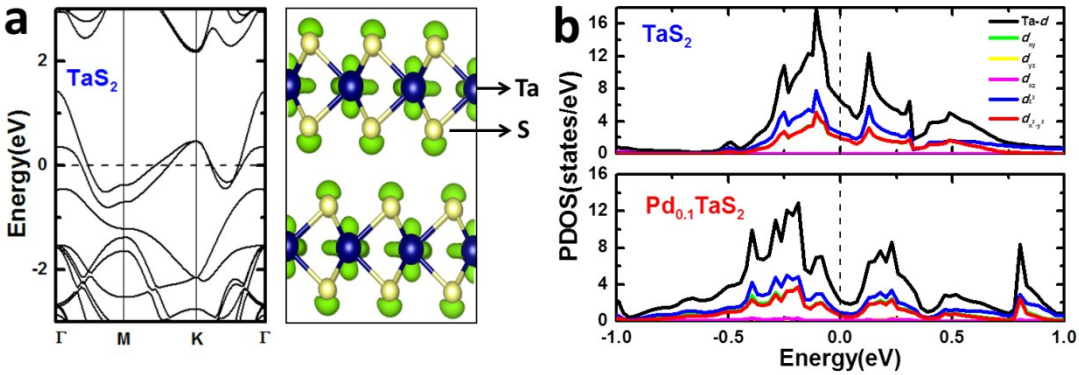

Figure S10. (**a**) Band structures and the partial charge density for electrons between −1.0 eV to Fermi level in TaS_2. The blue and white balls denote Ta and S, respectively. (**b**) The partial density of states of Ta−5*d* in 2H−TaS_2 and $Pd_{0.1}TaS_2$.

References for supplementary information:

[1] Jaramillo, T. F.; Jorgensen, K. P.; Bonde, J.; Nielsen, J. H.; Horch, S.; Chorkendorff, I., Identification of active edge sites for electrochemical H_2 evolution from MoS_2 nanocatalysts. *Science* **2007**, *317*, (5834), 100-102.

[2] Voiry, D.; Yamaguchi, H.; Li, J.; Silva, R.; Alves, D. C. B.; Fujita, T.; Chen, M.; Asefa, T.; Shenoy, V. B.; Eda, G.; Chhowalla, M., Enhanced catalytic activity in strained chemically exfoliated WS_2 nanosheets for hydrogen evolution. *Nat. Mater.* **2013**, 12, (9), 850-855.

[3] Jaramillo, T. F.; Bonde, J.; Zhang, J.; Ooi, B.-L.; Andersson, K.; Ulstrup, J.; Chorkendorff, I., Hydrogen evolution on supported incomplete cubane-type $[Mo_3S_4]^{4+}$ electrocatalysts. *J. Phys. Chem. C* **2008,** *112*, (45), 17492-17498.

[4] Qi, K.; Yu, S.; Wang, Q.; Zhang, W.; Fan, J.; Zheng, W.; Cui, X., Decoration of the inert basal plane of defect-rich MoS_2 with Pd atoms for achieving Pt-similar HER activity. *J. Mater. Chem. A* **2016**, *4*, (11), 4025-4031.

[5] Zeng, Z. Y.; Tan, C. L.; Huang, X.; Bao, S. Y.; Zhang, H., Growth of noble metal nanoparticles on single-layer TiS_2 and TaS_2 nanosheets for hydrogen evolution reaction. *Energ. Environ. Sci.* **2014**, *7*, (2),797-803.